

New possibilities for analyzing the biological role of hydrogen, methane and other biomarkers of gut microbiota activity using tunable diode laser absorption spectrometry and selective hydrogen and oxygen sensors

© Ya.Ya. Ponurovskii¹, D.B. Stavrovsky¹, I.V. Shirokov², F.I. Romanikhin², G.N. Bondarenko², A.V. Litvinov³, M.O. Etrekova³, A.A. Karabinenko⁴, V.A. Kilimnik⁵, O.S. Medvedev^{2,6}

¹ Prokhorov Institute of General Physics, Russian Academy of Sciences, 119991 Moscow, Russia

² Moscow State University, 119991 Moscow, Russia

³ National Research Nuclear University „MEPhI“, 115409 Moscow, Russia

⁴ Russian National Research Medical University named N.I. Pirogov, 117997 Moscow, Russia

⁵ Saint-Petersburg State University of Aerospace Instrumentation 190000 St. Petersburg, Russia

⁶ Smirnov Institute of Experimental Cardiology Chazov National Medical Research Center for Cardiology, 121552 Moscow, Russia

e-mail: jakov@nsc.gpi.ru

Received December 28, 2023

Revised January 17, 2024

Accepted March 05, 2024

The paper presents a hardware-software complex consisting of a multichannel tunable high-resolution diode laser spectrometer for measuring gases $^{12}\text{CO}_2$, $^{13}\text{CO}_2$, CH_4 , NH_3 , H_2S and H_2O , as well as hydrogen and oxygen sensors for *on-line* measurements of exhaled gases. It allows continuous (every second) non-invasive measurement of the composition of biomarkers of the intestinal microbiota both in experiments on laboratory animals and in clinical studies on humans. The first experiments showed the possibility of using the device to study both exhaled air and intestinal gas. An important advantage of the developed new method for recording gases is both the continuity of measuring the composition of gases and the multi-channel nature of the recorded components, which makes it possible to assess the characteristics of the enzymatic activity of the intestinal microbiota and indirectly judge its taxonomic composition

Keywords: hydrogen-methane breath test, water saturated with hydrogen and methane, oxidative stress, hydrogen sensor, diode laser multichannel spectrometer, diagnostics.

DOI: 10.61011/EOS.2024.03.58750.35-24

Introduction

Recent years have seen an upsurge in interest in studying the role of microorganisms of the large intestine (microbiota) of animals and humans and their capacity to generate a number of metabolites that may exert both protective and provocative influence on the development of metabolic, cardiovascular, and other non-infectious diseases [1]. The total number of microorganisms in the human body is 1.3–2.3 times (depending on the age and state of the body) higher than the total number of somatic cells [2]. The density of microbial cells is nonuniform along the gastrointestinal tract (GIT). It reaches its minimum of 10^2 – 10^3 microbial cells/ml in the stomach, which is apparently attributable to a high acidity; in the duodenum and upper parts of the small intestine, the level is 10^3 – 10^6 , which is associated with a relatively high rate of intestinal transit; in the lower parts of the small intestine, the level is 10^7 – 10^9 ;

the maximum density of 10^{10} – 10^{13} microbial cells/ml [3,4] is found in the colon.

Those food components (primarily complex carbohydrates and dietary fiber) that are not absorbed by our body in the small intestine reach the large intestine, where they are fermented by the microbiota with a much larger set of enzymes for their utilization. As a result of their metabolism, a large number of low-molecular-weight compounds are produced in the colon: gas biomarkers (hydrogen, methane, and hydrogen sulfide), short-chain fatty acids, etc. [5]. The rate of hydrogen formation in the intestine is related linearly to its level in exhaled air. Hydrogen produced as a result of fermentation of indigestible carbohydrates (i.e., those that are not absorbed in the small intestine) is absorbed into the blood. Approximately 21–65% of hydrogen formed in the intestine is released through the lungs, which is the basis for using the hydrogen

breath test for non-invasive assessment of the gas-forming function of the colon microbiota [6,7].

The hydrogen level in exhaled air is measured to determine ororectal transit time and diagnose small intestinal bacterial overgrowth (SIBO), lactase deficiency, and carbohydrate (fructose, galactose, sorbitol) intolerance [8,9]. However, a significant scatter of data, which does not allow one to define reference levels of hydrogen in air exhaled by a healthy person, is noted in most studies [10]. Guidelines for standardization of the procedure of hydrogen breath testing in a clinic and the interpretation of obtained data are being formulated on the basis of current research conducted in America and Europe [11,12]. It is especially important to implement continuous measurement of the level of hydrogen and methane when diagnosing SIBO, since the method relies on the notion of an earlier emergence of hydrogen or methane in exhaled air in the case of an increase in the number of microorganisms in the small intestine (when the bulk of the testing volume of carbohydrates has not yet reached the colon that contains much more microorganisms releasing a greater amount of gas than the one that may be formed in the small intestine) [6].

The exact time of detection of even small amounts of gas biomarkers in exhaled air is of particular importance in this context. Current methods for measuring the concentration of hydrogen and methane in exhaled air, which rely on the use of electrochemical sensors or gas chromatography, do not allow one to determine accurately the first signs of emergence of hydrogen or methane in exhaled air, since measurements are carried out once every 15 or 20 min (see the American [13], European [12], or Russian guidelines for performing a diagnostic test for SIBO). This temporal resolution is clearly insufficient to probe the initial phases of emergence of gas biomarkers in exhaled air. Almost continuous recording of the level of biomarkers is needed to raise the temporal accuracy of detection of their emergence in exhaled air. This may be achieved through the use of tunable diode laser absorption spectroscopy and a selective semiconductor hydrogen sensor. The aim of the present study was to design a hardware and software complex consisting of a multichannel high-resolution diode laser spectrometer for measuring the concentration of gaseous $^{12}\text{CO}_2$, $^{13}\text{CO}_2$, CH_4 , NH_3 , H_2S , and H_2O and hydrogen and oxygen sensors for *on-line* measurements of exhaled gases.

Materials and methods

An A3-05 multichannel diode laser spectrometer (DLS) was constructed based on instruments designed earlier for the measurement of gas mixtures in multi-pass Herriot cells [14,15]. Figures 1, *a* and *b* present the schematic block diagram of the A3-05 DLS and the photographic image of the spectrometer. Laser radiation unit 1, which operates at wavelengths with tuning in the vicinity of absorption lines of detected molecules, features diode laser module 5, fiber

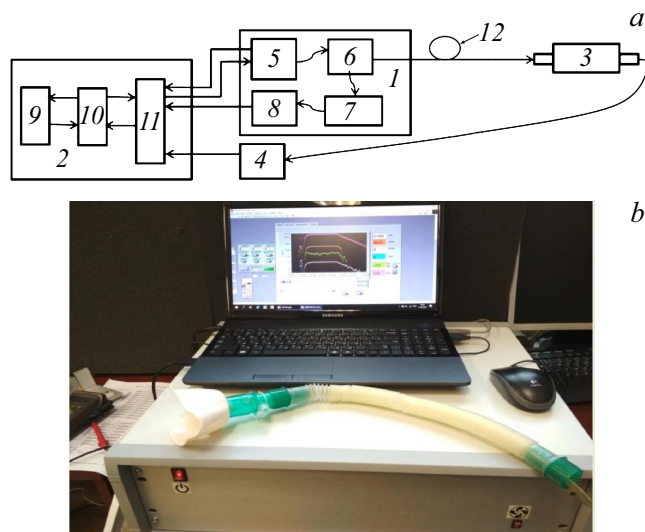


Figure 1. *a* — Schematic block diagram of the A3-05 DLS; *b* — photographic image of the spectrometer.

splitter 6 used to feed laser radiation into a transmit-receive channel and a reference channel, reference cells with Fabry–Pérot interferometer 7, and comparison signal detector 8. Control, reception, and data processing unit 2 is designed in the form of three modules: digital programmable module 9, module 10 of digital-to-analog and analog-to-digital converters (DACs and ADCs), and analog signal converter module 11. Multi-pass optical cell 3 and analytical signal detector 4 are used to measure gas concentrations. This cell has the following parameters: cell type — Herriot; base length — 30 cm; total optical path length — 28 m; volume — 21. The cell is vacuum-sealed and made of stainless steel. Module 5 is a near-IR diode laser (DL) with distributed feedback and radiation output into a single-mode fiber. Three tunable diode lasers with distributed feedback operating at a wavelength of 1.651, 1.512, and 1.604 μm (LD-PD INC, Singapore; <http://ld-pd.com/>) are used in the instrument. The 20-cm-long reference cell is made of heat-resistant glass and is used as a comparison element in calculation of the gas concentration. It was filled with studied CH_4 , CO_2 , H_2S , and NH_3 gases at partial pressures of 30, 100, 75, and 35 Torr, respectively. The total pressure of gases in the cell when diluted with nitrogen was 350 Torr. Detectors 4 (of the analytical signal) and 8 (of the comparison signal) are InGaAs pin photodiodes with an active area diameter of 2 mm (Beijing Lightsensing Technologies Ltd, China; <http://en.lightsensing.com>). Fiber optic cable 12 is a quartz single-mode fiber light guide with optical radiation losses no worse than 0.25 dB/km at a wavelength of 1.55 μm . Digital programmable module 9 and DAC and ADC module 10 are constructed based on a USB-6343 multifunction input/output device (National Instruments, United States; <https://www.ni.com>).

In response to a command from digital programmable module 9 and DAC and ADC module 10, diode laser 5

generates a sequence of short pulses at a wavelength matching the absorption line of the detected gas. Pump current pulses of the diode laser are trapezoidal with a duration of 1–4 ms and a repetition rate no greater than 200 Hz. They allow for additional radiation scanning around the center of the absorption line needed to cover the entire line profile and ensure high selectivity for the chosen gas component. Comparison signal detector 8 is used to tune the device: set a given wavelength range for the diode laser emitter by adjusting the temperature of the Peltier thermoelement on which the diode laser is positioned. The Peltier thermoelement current is controlled by digital programmable module 9 through DAC and ADC module 10 and analog signal converter module 11. The electrical signal from the Peltier temperature sensor enters digital programmable module 9 through analog signal converter module 11 and DAC and ADC module 10. The major part of diode laser radiation from the fiber splitter enters fiber optic cable 12 and is fed to the input of multi-pass optical cell 3. Diode laser radiation leaving the cell is collimated onto the photodetector of the analytical signal detector. The detector signal is then amplified and digitized (10, 11), and the concentration of the detected gas is calculated using digital programmable module 9. Technical parameters of the A3-05 DLS are listed in the table.

Gas concentration measurement

The HITRAN-2020 [16] spectral database was used to model absorption spectra and choose the optimum spectral ranges for detection of impurities in exhaled gases. According to the Bouguer–Lambert law, intensity $I(\nu)$ of radiation at frequency ν absorbed in a medium is related to intensity $I_o(\nu)$ of incident radiation, absorption coefficient $\kappa(\nu)$, gas concentration c , and path length l by the following formula:

$$I(\nu) = I_o(\nu) \exp(-\kappa(\nu)cl), \quad (1)$$

where absorbance $D^*(\nu) = \kappa(\nu)cl$.

The profile of absorption coefficient $\kappa(\nu)$ depends on broadening of the line of absorption of the molecule by the buffer gas (in the present case, the atmosphere) and is Lorentzian in shape:

$$\kappa(\nu) = S_{ij}f(\nu - \nu_o), \quad (2)$$

$$f(\nu - \nu_o) = (b_l/\pi)/((\nu - \nu_o)^2 + b_l^2), \quad (3)$$

where S_{ij} is the intensity of the vibrational-rotational line at which laser radiation is absorbed. Spectral parameters of the vibrational-rotational molecular line (intensity S_{ij} , frequency ν_o , Lorentzian collisional half-width b_l) for absorption spectra modeling were taken from the HITRAN spectral database. The chemical composition of samples of exhaled gases was determined: $\text{CO}_2 = 40000$ ppm, $\text{H}_2\text{O} = 2\%$, $\text{CH}_4 = 2.5$ ppm, $\text{NH}_3 = 0.50$ ppm, $\text{H}_2\text{S} = 0.2$ ppm, total pressure = 630 Torr, $T_{\text{air}} = 35^\circ$; model absorption spectra of these gases in the diode laser region were plotted, and

analytical spectral regions of gas detection were identified. In the case of $^{12}\text{CO}_2$, $^{13}\text{CO}_2$, H_2S , and H_2O , this is the (6232.5–6235.2 cm^{-1}) range; the (6054.2–6059 cm^{-1}) range corresponds to CH_4 ; and (6611.5–6613.6 cm^{-1}) is the range for NH_3 and H_2O .

Algorithm for concentration measurements under amplitude modulation of the diode laser pump current

The diode laser frequency was tuned by periodic pump current pulses of a special (trapezoidal) shape with a duration of 1–4 ms and a repetition rate of 60 Hz, which were discussed in detail in [17]. A pump current pulse was modulated in amplitude with a frequency equal to the sampling frequency of the ADC of NI USB-6343. The bandwidth of preamplifiers of the photodetectors of analytical channels was optimized for the sampling frequency and was set to 111 kHz. The amplitude modulation depth was selected in such a way as to provide a frequency shift of laser radiation by a half-width of the gas absorption lines and the maximum absorption contrast.

Mathematical processing of amplitude-modulated signals was then carried out:

- 1 — logarithmation of frequency-shifted signal components in accordance with the Beer–Bouguer–Lambert law;
- 2 — autocorrelation convolution of the reference signal R_{xx} and cross-correlation convolution of the reference signal with the analytical one R_{xy} (this provides additional filtering of the noisy target signal);
- 3 — linear fitting of the cross-correlation function to the autocorrelation function and determination of their match factor α :

$$R_{xy} = \alpha R_{xx}. \quad (4)$$

Match factor α is proportional to unknown concentration C of the studied gas, which is determined as

$$C = \frac{\alpha P_R L K_R}{P_A L_A} \cdot 10^2, \quad (5)$$

where C is the concentration of the studied gas in percent; P_R, P_A are the partial gas pressures in the reference and analytical channels, respectively; and L_R, L_A are the optical lengths of the reference and multi-pass cells, respectively. The presented procedure for concentration calculation provides for a marked suppression of low-frequency noise of various nature (vibration, flicker) in the receiving and recording path of the A3-05 DLS [18].

Hydrogen and oxygen sensors

An MIS (metal–insulator–semiconductor) structure of the Pd-SiO₂-Si type is used as a sensitive element in the hydrogen gas analyzer. The electrical capacitance of this structure changes on interaction with gas [19]. The method of fabrication of this sensing element is a combination

Technical specifications of the A3-05 DLS

№.	Parameter	Parameter value
1	Spectral range of concentration measurement $^{12}\text{CO}_2$, $^{13}\text{CO}_2$, CH_4 , NH_3 , H_2S , H_2O	1.28–1.65 μm
2	DL radiation power, lower than	10 mW
3	Radiation frequency stability, no worse than	0.0005 cm^{-1}
4	Spectral resolution, no worse than	0.0004 cm^{-1}
5	Absolute error of concentration measurements/measurement range $^{12}\text{CO}_2$ $^{13}\text{CO}_2$ CH_4 NH_3 H_2S H_2O	20 ppm* /0–20% 20 ppm /0–20% 0.2 ppm /0–1% 0.01 ppm /0–50 ppm 0.7 ppm /0–20 ppm 0.01% /0–100%
7	Gas concentration measurement time, no greater than	100 ms
8	Size, no greater than	45 cm(W)×27 cm(L)×20 cm(H)
9	Weight, no greater than	8.0 kg
10	Power consumption, no greater than	120 W

Note. * ppm — one part per million (million^{-1}).

Basic technical specifications of the hydrogen sensor:

Concentration range	0.1–1000 ppm,
Response time	0.1–5 min,
Operating temperature	140°C,
Service life	5 years.

Basic technical specifications of the oxygen sensor:

Concentration range	0.1–30%,
Response time	3–12 s,
Operating conditions	$T = -35 + 50^\circ\text{C}$,
Pressure	630–800 Torr,
Service life	4 years.

of microelectronic transistor technology and laser thin-film deposition. The MIS sensor is designed based on a capacitor structure consisting of a silicon wafer, a dielectric SiO_2 layer, and a palladium metal electrode (gate). The electrical capacitance of this capacitor is C . Its temperature is maintained within the 100–150°C range using a miniature resistive film heater and stabilized by an electronic unit with a thermistor. The sensor operates in the following way. When molecules of the gas under study are deposited onto the gate (Pd) surface, the $C-U$ characteristic shifts along the U axis. With constant voltage U_{cm} maintained across the capacitor, a change in capacitance ΔC is observed and converted by the electronic unit into an analog (or digital) signal [20].

A commercial „Oksik-3“ electrochemical sensor produced by LLC „Oxonium“ (St. Petersburg; <http://www.oxonsens.ru/>) was used to measure the oxygen concentration. This sensor operates based on the variation of electrical voltage that is proportional to the partial pressure of oxygen in air in the working area. The sample interacts with the sensor via diffusion penetration of a gas mixture.

Results and discussion

A special sealed system for air intake and filtration into the multi-pass cell of the A3-05 DLS and O_2 and H_2 sensors was designed for examining the gas composition of exhaled air. Three micropumps were used to route test air flows into the multi-pass cell, the hydrogen sensor, and the oxygen sensor. The air flow rate in each channel was regulated by flow meters. An individual carbon filter was installed for the hydrogen sensor to remove moisture, ammonia vapor, and hydrogen sulfide. To prevent pressure surges and ensure a continuous laminar supply of air into the multi-pass cell, an additional buffer volume with pressure relief valves was introduced. The multi-pass cell was made vacuum-sealed to ensure leak-tightness of the entire inlet system and to prevent atmospheric air feeding from the flanges of mirrors, valves, etc.

Pilot testing of the developed system was carried out on rats to record the moment of release of intestinal gases from the colon. The rear part of a rat body was introduced into a sealed plexiglass case that was ventilated with air at a rate of 2 l/min. Gas leaving the case entered the air

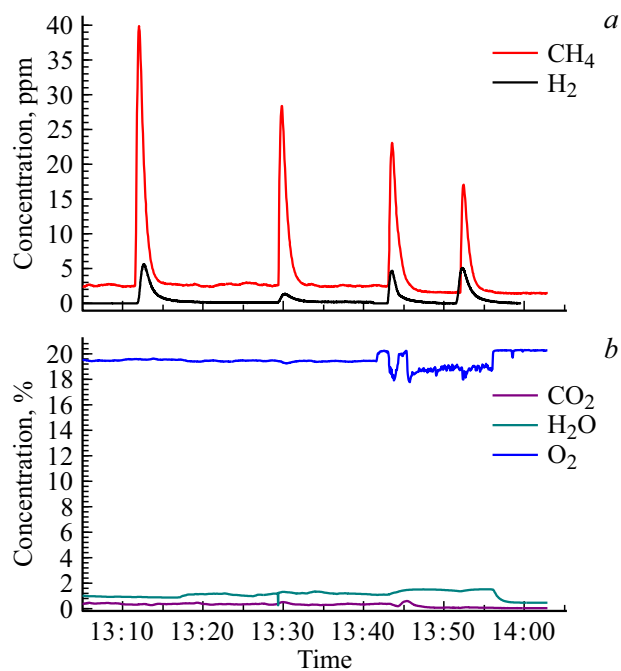


Figure 2. Detection of intestinal gases of a rat: *a* — variations of the CH₄ and H₂ concentration, *b* — variations of the CO₂, H₂O, and O₂ concentration.

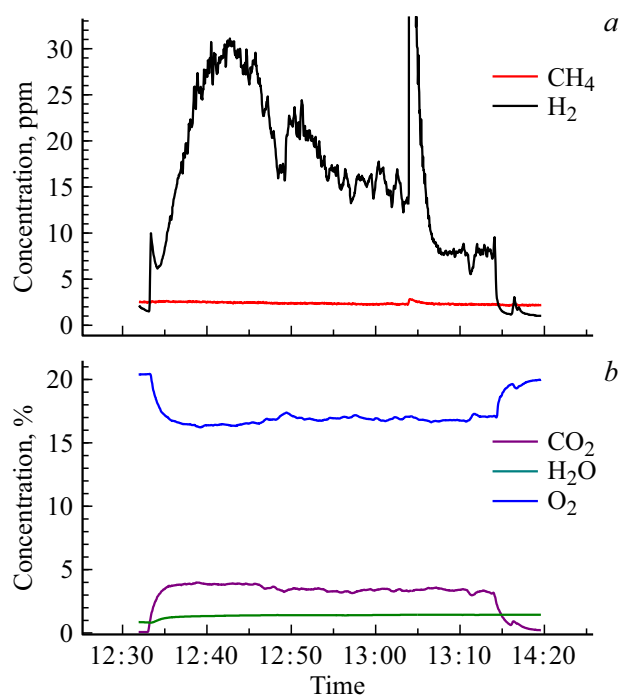


Figure 3. Breath test of a person who drank a glass of hydrogen-saturated water: *a* — variations of the CH₄ and H₂ gas concentration, *b* — variations of the CO₂, H₂O, and O₂ gas concentration.

supply system and was fed to the multi-pass cell and H₂ and O₂ sensors. A typical result of these experiments is presented in Fig. 2. It is evident that the concentrations

of hydrogen and methane spiked at different time intervals, indicating the presence of both hydrogen-generating bacteria and methane-generating microorganisms in the microbiota. As other rats were tested, individuals with selective release of intestinal gas containing hydrogen only were identified. Thus, continuous recording of the composition of intestinal gases allows one to assess differences in the composition of microorganisms in the microbiota non-invasively.

Pilot studies in humans were performed on three healthy volunteers of different age (25–80 years). Air exhaled by a person was drawn in continuously through a sealed breathing mask fitted with inspiratory–expiratory valves. Exhaled air was then fed through the filtration and supply system to the measuring channels of the A3-05 laser spectrometer. Following 10-minute recording of background levels of gases in exhaled air, the subject drank a glass of water (200 ml) saturated with hydrogen (the hydrogen concentration in water ranged from 1.0 to 1.4 ppm). The measurement of exhaled gases continued for 40 min. Figure 3 presents the experimental data for a person who drank a glass of hydrogen-saturated water.

A reduction in oxygen concentration and an increase in carbon dioxide concentration allow one to estimate the so-called respiratory coefficient (i.e., metabolic features of a particular individual: the degree of metabolism of fats or carbohydrates). Hydrogen from the ingested water is absorbed quickly into the blood and released through the lungs.

The concentration of hydrogen peaks 10–12 min after ingestion of water, and hydrogen is removed completely from the body in 45–60 min. Since all the blood supplying the human gastrointestinal tract enters through the portal vein into the liver, a possibility emerges to assess the degree of uptake of hydrogen, which has antioxidant properties, by the liver and, consequently, evaluate indirectly the degree of oxidative stress in liver tissue [21].

Conclusion

The tunable diode laser spectrometer discussed above makes it possible to measure continuously (every second) and non-invasively the composition of biomarkers of the intestinal microbiota both in experiments on laboratory animals and in clinical studies on humans. The initial experiments revealed that the device is suitable for examination of both exhaled air and intestinal gas. The continuity of measurements of the gas composition and the multichannel capacity, which makes it possible to assess the features of enzymatic activity of the intestinal microbiota and evaluate its taxonomic composition indirectly, are both important advantages of the developed method.

Compliance with ethical standards

All applicable international, national, and/or institutional guidelines for animal care and management were observed.

All procedures performed in studies involving human participants were in accordance with the ethical standards of the institutional and/or national research committee and with the 1964 Helsinki Declaration and its later amendments or comparable ethical standards.

Funding

The development of a multichannel DL spectrometer and a hydrogen sensor and hydrogen–methane breath testing were supported by grant No. 19-19-00712 from the Russian Science Foundation.

Conflict of interest

The authors declare that they have no conflict of interest.

References

- [1] R. Singh, J. Fedacko, O. Medvedev, T. Truong, T. Kuropatkina, L. Shogenova, S. Chibisov, G. Halabi, E. Kharlitskaya, G. Ak-BawareedElkilany, O. Elmarghi. *World Heart Journal*, **14** (4), 305 (2022).
- [2] R.C. Robertson, A.R. Manges, B.B. Finlay, A.J. Prendergast. *Trends Microbiol.*, **27** (2), 131 (2019). DOI: 10.1016/j.tim.2018.09.008
- [3] M. Mailhe, D. Ricaboni, V. Vitton, J.-M. Gonzalez, D. Bachar, G. Dubourg, F. Cadoret, C. Robert, J. Delerce, A. Levasseur, P.-E. Fournier, E. Angelakis, J.-C. Lagier, D. Raoult. *BMC Microbiol.*, **18** (2), 157 (2018). DOI: 10.1186/s12866-018-1304-7
- [4] O.S. Medvedev. *Usp. Sovrem. Biol.*, **142** (4), 349 (2022) (in Russian). DOI: 10.31857/S004213242204007X
- [5] K. Kalantar-Zadeh, K.J. Berean, R.E. Burgell, J.G. Muir, P.R. Gibson. *Nat. Rev. Gastroenterol. Hepatol.*, **16** (12), 733 (2019). DOI: 10.1038/s41575-019-0193-z
- [6] M.D. Levitt, N. Engl. J. Med., **281** (3), 122 (1969). DOI: 10.1056/NEJM196907172810303
- [7] S.U. Christl, P.R. Murgatroyd, G.R. Gibson, J.H. Cummings. *Gastroenterology*, **102** (4 Pt 1), 1269 (1992).
- [8] W. Shin. *Anal. Bioanal. Chem.*, **406** (16), 3931 (2014). DOI: 10.1007/s00216-013-7606-6
- [9] E.A. Kornienko, S.S. Kubalova, M.A. Dmitrienko, I.E. Dzhatspanyan. *Pediatrics*, **4** (1), 9 (2013) (in Russian).
- [10] M. Di Stefano, C. Mengol, M. Bergonzi, E. Pagani, G.R. Corazza. *Eur. Rev. Med. Pharmacol. Sci.*, **17** (Suppl 2), 36 (2013).
- [11] A. Rezaie, M. Buresi, A. Lembo, H. Lin, R. McCallum, S. Rao et al. *Am. J. Gastroenterology*, **112** (5), 775 (2017). DOI: 10.1038/ajg.2017.46
- [12] H.F. Hammer, M.R. Fox, J. Keller, S. Salvatore, G. Basile, J. Hammer et al. *United European Gastroenterol. J.*, **10** (1), 15 (2022). DOI: 10.1002/ueg2.12133
- [13] M. Pimentel, R.J. Saad, M.D. Long, S.S. Rao. *Am. J. Gastroenterol.*, **115** (2), 165 (2020). DOI: 10.14309/ajg.0000000000000501
- [14] A.I. Nadezhdinskii, Ya.Ya. Ponurovskii. *Quant. Electron.*, **49** (7), 613 (2019). DOI: 10.1070/QEL16776
- [15] A.I. Nadezhdinskii, Ya.Ya. Ponurovskii. *Phys. Wave Phenom.*, **26**, 169 (2018). DOI: 10.3103/S1541308X18030019
- [16] I.E. Gordon, L.S. Rothman, R.J. Hargreaves et al. *JQSRT*, **277**, 107949 (2020). DOI: 10.1016/j.jqsrt.2021.107949
- [17] M.A. Bolshov, Yu.A. Kuritsyn, V.V. Liger, V.R. Mironenko, Ya.Ya. Ponurovskii. *J. Anal. Chem.*, **78** (10), 1281 (2023). DOI: 10.1134/S1061934823100052
- [18] A.I. Nadezhdinskii, Y.Y. Ponurovskii. *Laser Phys.*, **33** (5), 55001 (2023). DOI: 10.1088/1555-6611/acc23d
- [19] B.A. Bolodurin, V.Yu. Korchak, A.V. Litvinov, A.A. Mikhailov, D.A. Nozdrya, Yu.V. Pomazan, D.V. Filipchuk, M.O. Etrekova. *Russian J. General Chemistry*, **88**, 2732 (2018). DOI: 10.1134/S1070363218120435
- [20] A. Litvinov, N. Samotaev, M. Etrekova, A. Ivanova, D. Filipchuk. *J. Electrochem. Soc.*, **168**, 017503 (2021). DOI: 10.1149/1945-7111/abd5fb
- [21] A. Shimouchi, K. Nose, M. Shirai, T. Kondo. *Adv. Exp. Med. Biol.*, **737**, 245 (2012). DOI: 10.1007/978-1-4614-1566-4_36

Translated by D.Safin